Drug Metabolism Letters, 2021, *14*, 206-218

RESEARCH ARTICLE

Comparative *In vitro* Metabolism of Enflicoxib in Dogs, Rats, and Humans: Main Metabolites and Proposed Metabolic Pathways

Josep Solà[1], Àngel Menargues[1], Josep Homedes[2,*], Marta Salichs[2], Maria Teresa Serafini[3] and Gregorio Encina[3]

[1]*Experimental Toxicology and Ecotoxicology Unit (CERETOX), Barcelona Science Park, Barcelona, Spain;* [2]*Ecuphar Veterinaria S.L.U. (Animalcare Group PLC), Barcelona, Spain;* [3]*Welab Barcelona, Barcelona Science Park, Barcelona, Spain*

Abstract: ***Background*:** Enflicoxib is a non-steroidal anti-inflammatory drug of the coxib family characterized by a long-lasting pharmacological activity that has been attributed to its active metabolite E-6132.

***Objectives*:** The aim of this work was to explore enflicoxib biotransformation *in vitro* in humans, rats and dogs, and to determine its metabolic pathways.

***Methods*:** Different *in vitro* test systems were used, including hepatocytes and liver and non-hepatic microsomes. The samples were incubated with enflicoxib and/or any of its metabolites at 37°C for different times depending on the test system. The analyses were performed by liquid chromatography coupled with either radioactivity detection or high-resolution mass spectrometry.

***Results*:** Enflicoxib was efficiently metabolized by cytochrome P-450 into three main phase I metabolites: M8, E-6132, and M7. The non-active hydroxy-pyrazoline metabolite M8 accounted for most of the fraction metabolized in all the three species. The active pyrazol metabolite E-6132 showed a slow formation rate, especially in dogs, whereas metabolite M7 was a secondary metabolite formed by oxidation of M8. In hepatocytes, diverse phase II metabolite conjugates were formed, including enflicoxib glucuronide, M8 glucuronide, E-6132 glucuronide, M7 glucuronide, and M7 sulfate. Metabolite E-6132 was most probably eliminated by a unique glucuronidation reaction at a very low rate.

***Conclusion*:** The phase I metabolism of enflicoxib was qualitatively very similar among rats, humans and dogs. The low formation and glucuronidation rates of the active enflicoxib metabolite E-6132 in dogs are postulated as key factors underlying the mechanism of its long-lasting pharmacokinetics and enflicoxib's overall sustained efficacy.

ARTICLE HISTORY

Received: September 13, 2021
Revised: November 03, 2021
Accepted: November 16, 2021

DOI:
10.2174/1872312814666211209161933

Keywords: Enflicoxib, metabolism, CYP, COX-2, dog, rat, humans.

1. INTRODUCTION

Enflicoxib is a newly approved non-steroidal anti-inflammatory drug of the coxib family intended for the treatment of pain and inflammation associated with osteoarthritis in dogs [1]. Enflicoxib has shown potent anti-inflammatory and analgesic properties *in vivo* in several experimental models of inflammation and pain [2]. Its mechanism of action is based on a strong inhibition of the cyclooxygenase enzyme, showing high selectivity for its inducible form, COX-2 [3].

Enflicoxib(4-(5-(2,4-difluorophenyl)-3-(trifluoromethyl)-4,5-dihydro-1H-pyrazol-1-yl) benzenesulfonamide) belongs to the sulphonamide chemical family with a diaryl-substituted pyrazoline structure containing a sulfamoylphenyl group Fig. (**1A**) that is thought to be indispensable for its COX-2 inhibitory activity [4, 5]. Furthermore, enflicoxib is a racemic molecule with one chiral center that shows an equal proportion of its two enantiomers: (R)-(+)-enflicoxib and (S)-(-)-enflicoxib (also known as E-6231 and E-6232, respectively [6]). E-6232 has been demonstrated as the active enantiomer, while the pharmacological activity of E-6231 is negligible. In addition, a non-chiral pyrazol metabolite of enflicoxib (namely E-6132, Fig. (**1B**)) was identified earlier, which also exerts a potent and selective inhibitory effect on COX-2 [3]. Following enflicoxib administration to dogs, the E-6132 metabolite shows a longer half-life and higher volume of distribution than the parent compound and is believed to account for most of the long-lasting pharmacological activity of enflicoxib [1, 7, 8]. Besides E-6132, the chem-

*Address correspondence to this author at the Ecuphar Veterinaria S.L.U. (Animalcare Group PLC), Barcelona, Spain; E-mail: jhomedes@ecuphar.es

ical structure of another phase I metabolite (M8) has also been identified, which corresponds to a hydroxylated pyrazoline derivative of enflicoxib [9] Fig. (**1C**). Metabolite M8 displays no inhibitory effect on COX-1 or COX-2.

During the early developmental phases of a new drug candidate, *in vitro* metabolism studies provide essential information for valuable foresight on metabolic pathways in the target species and for the selection of the most suitable species for toxicological evaluation. Several *in vitro* test systems are commonly used for this purpose, such as hepatocytes and liver and non-hepatic microsomes. The purpose of this work was to explore the metabolite profile and the metabolic pathways of enflicoxib as well as potential differences among dogs (as the target clinical species), rats (as preclinical species), and humans (to extrapolate toxicity studies in the context of user risk assessment) [10].

2. MATERIALS AND METHODS

2.1. Reference Standards, Reagents and Biologic Material

Racemic enflicoxib (molecular weight 405.34; purity 100%) was synthesized by Esteve Pharmaceuticals (Barcelona, Spain); metabolite M8 (two batches of the racemic (-)anti diastereoisomer, molecular weight 421.05; purity 97.6% and 98.9%) was synthesized by Esteve Pharmaceuticals and by GalChimia (A Coruña, Spain); and pyrazol metabolite E-6132 (molecular weight 403.33; purity 99.03%) was synthesized by GalChimia. [^{14}C]Enflicoxib (specific activity 33.2 μCi/mg; radiochemical purity >99%) was custom-labeled by BioDynamics (Billingham, UK). Working solutions of substrates and metabolites were prepared in dimethylsulfoxide (DMSO). All reagents, including enzyme cofactors and positive metabolism controls, were purchased from Merck Sigma-Aldrich (St. Louis, MO, USA), except where otherwise indicated. Reagents used for HPLC analysis were of analytical or liquid chromatography-mass spectrometry (LC-MS) grade. Biologic material was purchased from accredited suppliers. Pooled liver microsomes and cryopreserved hepatocytes from male beagle dogs and Wistar rats, together with intestinal microsomes from male Sprague-Dawley rats and beagle dogs, were purchased from BioIVT (Westbury, NY, USA). Human liver microsomes pooled from male and female donors were purchased from Sekisui Xenotech LLC (Kansas City, KS, USA) and Biopredic (Rennes, France).

2.2. Metabolism of [^{14}C]Enflicoxib in Liver Microsomes from Dogs, Rats and Humans

Liver microsomes (microsomal protein: 1 mgmL^{-1}) from male Wistar rats, male beagle dogs and humans (pool of both genders) were incubated in duplicate with 20 μM [^{14}C]Enflicoxib as substrate at 37°C in phosphate buffer (pH 7.4) containing $MgCl_2$. [^{14}C]Enflicoxib working solutions were prepared in DMSO, with its concentration in the final incubates being 1%. Incubations were performed in the presence of an NADPH-generating system. The reactions were started by adding NADP and were quenched at 0, 30, 60 and 90 min by adding two volumes of acetonitrile. Samples without [^{14}C]Enflicoxib, without NADP and without microsomes were prepared to check enzymatic reactions and to assess substrate stability at 37°C. The samples generated were centrifuged and the supernatants were directly analyzed by high-performance liquid chromatography with on-line radioactivity detection (HPLC-rad).

2.3. Assessment of the Enflicoxib Metabolism in Rat and Dog Intestinal Microsomes

Intestinal microsomes (microsomal protein: 2 mgmL^{-1}) from male Sprague-Dawley rats and male beagle dogs were incubated in duplicate with 20 μM unlabeled enflicoxib at 37°C in phosphate buffer (pH 7.4) containing $MgCl_2$. Enflicoxib working solutions were prepared in DMSO, with itsconcentration in the final incubates being 1%. The reactions were started by adding 1 mM NADPH and were quenched at 0, 60 and 120 min by adding one volume of methanol containing 0.2% formic acid (FA). Samples without enflicoxib,

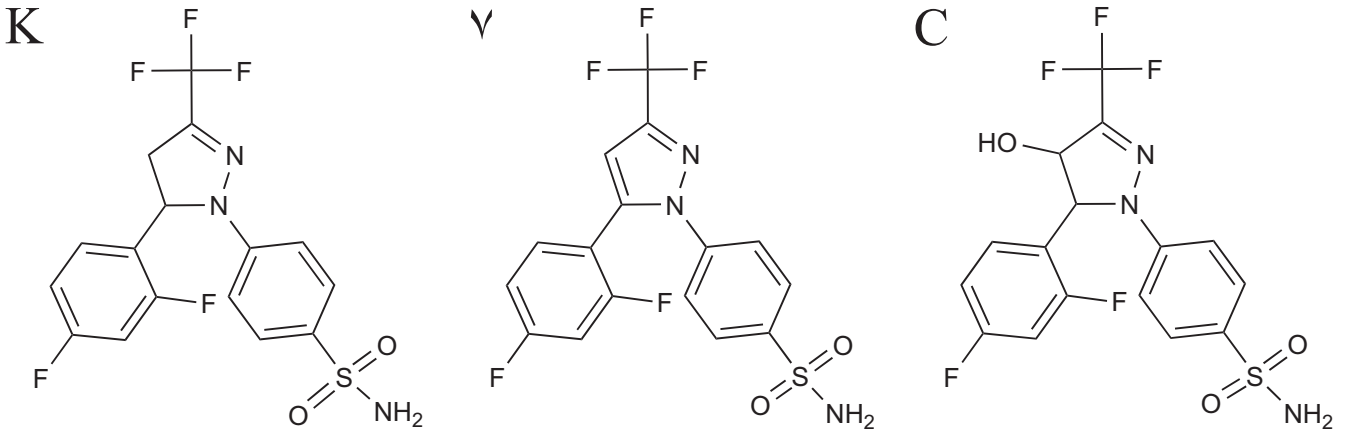

Fig. (1). Chemical structures of enflicoxib (**A**) and its metabolites: E-6132 (pyrazol metabolite), (**B**) and M8 (hydroxyl-pyrazoline metabolite), (**C**).

without NADPH and without microsomes were prepared to check enzymatic reactions, and to assess substrate stability at 37°C. Metabolic control incubations with the CYP substrate testosterone (10 μM) were performed at T=0 and 10 min to validate the experimental system. The samples generated were directly analyzed by LC-MS after centrifugation at 5.000 x *g* at 4°C for 15 min. Enflicoxib and metabolites E-6132 and M8, together with the metabolic controls, were quantified by LC-MS using reference standards.

2.4. Assessment of the Secondary Phase I and Phase II Metabolism of Enflicoxib in Liver Microsomes and Hepatocytes

Liver microsomes (microsomal protein: 1 $mgmL^{-1}$) from male Wistar rats and male beagle dogs were incubated in duplicate with 20 μM unlabeled enflicoxib or its metabolites E-6132 and M8 at 37°C in phosphate buffer (pH 7.4) containing $MgCl_2$ and NADPH, as described in the former section. Incubations were performed for 0, 60 and 120 min.

Cryopreserved hepatocytes from the same species and sex were thawed following the supplier´s recommendations. After thawing, the cells were counted, and their viability was measured using the trypan blue exclusion method. The hepatocyte viability was 86% for the dog and 85% for the rat (above the acceptance criteria of the supplier, *i.e*., >70%). Hepatocytes were re-suspended in William's E medium without phenol red, and the cell density was adjusted to 1 x 10^6 viable hepatocytes mL^{-1}. Incubations were performed separately with 20 μM unlabeled enflicoxib or E-6132 metabolite for 0, 120 and 180 min.

For all incubations, the substrate working solutions were prepared in DMSO, with its final concentration in the incubates being 1%. The reactions were quenched by adding one volume of methanol containing 0.2% FA. Samples without substrate (*i.e*., enflicoxib, E-6132 or M8), without NADPH (for microsomes), and without microsomes or hepatocytes, were prepared to check enzymatic reactions and to assess substrate stability at 37°C. Positive metabolism control incubations with the cytochrome P-450 (CYP) substrate testosterone and the UDP-glucuronosyl transferase substrate 4-methyl-7-hydroxycoumarin, both at 10 μM, were run at T=0 and 10 or 30 min for liver microsomes and hepatocytes, respectively. The samples generated were directly analyzed by LC-MS after centrifugation at 5.000 x *g* at 4°C for 15 min.

2.5. Characterization of the Metabolic Pathway of M7 Formation

The potential secondary phase I transformation of metabolites M8 and E-6132, and the possible pathway of metabolite M7 formation were assessed in incubations of dog and rat liver microsomes with 20 μM M8 or E-6132. The incubations were performed with 1 $mgmL^{-1}$ microsomal protein concentration for 0, 60 and 120 min in the presence of NADPH cofactor. The working solutions of M8 or E-6132 were prepared in DMSO, with the concentration in the final incubates being 1% v/v. The samples were analyzed by LC-MS using targeted high-resolution MS detection, and the results were expressed as peak areas. The phase I metabolic positive control testosterone was used to validate the experiments.

The chemical structure of metabolite M7 was tentatively identified by high resolution mass spectrometry. Detailed descriptions of the experimental and analytical parts are included as supplementary material in this article.

2.6. HPLC Analysis with On-line Radioactivity Detection

[^{14}C]Enflicoxib and its labeled metabolites were separated at room temperature using two Inersil ODS-3V columns (5 μm, 0.46 x 15 cm) with a Tracer CIS pre-column, a 515 pump and a 717 plus autosampler (Waters, Milford, MA, USA). The mobile phase consisted of 10 mM ammonium formate, pH 3 (A), and acetonitrile (B), and the flow rate was 1 $mLmin^{-1}$. The initial mobile phase contained 20% B that was increased linearly up to 50% over the next 30 min. The percentage of B was maintained at 50% until minute 80, increased to 75% over 10 min, and then maintained at this level for 5 minutes. Radiochemical detection was performed on-line using a Packard 500TR radioflow detector equipped with a liquid scintillation flow cell (Perkin Elmer, Waltham, MA, USA). Ultima-Flo^{TM} scintillation cocktail (Perkin Elmer) was pumped at a 2:1 (v/v) rate with respect to the HPLC eluent. Ultra-violet absorbance (UV) peaks were detected using a Waters 996 photodiode array (PDA) detector.

2.7. LC-MS Analysis of Sample Incubates with Unlabeled Compounds

Enflicoxib and its metabolites were separated at 40°C in a Kinetex F5 HPLC column (2.6 μm, 100 x 3.0 mm, Phenomenex, Torrance, CA, USA) using a Waters Alliance 2695 HPLC system. The mobile phase consisted of water containing 0.1% FA (A) and methanol (B), and the flow rate was 0.75 $mLmin^{-1}$. The initial mobile phase contained 20% B that was increased linearly up to 70% over 10 min. The percentage of B was rapidly changed to 90% in 0.5 min and maintained at this level for two minutes. MS detection was performed in an LTQ-Orbitrap Velos mass spectrometer (Thermo Scientific, Waltham, MA, USA) operating in negative ionization mode (Ion Max ESI Source). The ion spray voltage and the source temperature were -3300 V and 320°C, respectively. The fragmentation method was collision-induced dissociation (CID) for targeted analysis with variable collision energies depending on the analyte. The collision gas was helium, and the fragmentation and detection were at the lineal ion trap (LTQ).

Positive metabolism controls, testosterone and 4-methyl-7-hydroxycoumarin, and their respective internal standards, dexamethasone and 7-hydrocycoumarin, were separated in a Synergi Polar-RP column (4 μm, 50 x 2 mm, Phenomenex) at 40°C. The mobile phase consisted of water containing 0.1% FA (A) and acetonitrile (B), and the flow rate was 0.5 $mLmin^{-1}$. The mobile phase was pumped in gradient mode. MS detection was performed in the LTQ-Orbitrap Velos mass spectrometer operating in positive ionization mode for targeted analysis with variable collision ener-

gies depending on the analyte. The ion spray voltage and the source temperature were 4500 V and 320°C, respectively.

2.8. Calculations

For the HPLC-rad analyses, the chromatographic peaks were integrated, and the relative percentages of each labeled compound were obtained with respect to total radioactivity. The concentrations of unchanged enflicoxib and its metabolites were determined from the percentage data considering the nominal substrate concentration and the incubation volume. In the samples analyzed by LC-MS, the concentrations of enflicoxib, M8 and E-6132 were determined by calibration with authentic standards. Quantitative concentration data for metabolite M7 could not be obtained due to the lack of a reference standard, and the results are reported as LC-MS peak area.

The rates of enflicoxib biotransformation and metabolite formation were calculated from the concentrations obtained at the different incubation times. To this end, the slope of the linear fit of analyte concentration versus time during the linear phase of elimination or formation was calculated and expressed as pmol min^{-1} mg^{-1} for microsome incubations and as pmol $(min \cdot 10^6 \text{ cells})^{-1}$ for hepatocyte incubations. Substrate transformation was previously checked for linearity with respect to the selected microsomal protein or cell density ranges.

The log percentage of substrate remaining versus time was plotted for the positive metabolism controls, and the slope of the resulting linear regression (-*k*) was used to obtain *in vitro* $t_{1/2}$ (*in vitro* $t_{1/2} = 0.693/k$).

3. RESULTS

3.1. *In vitro* Metabolism of Enflicoxib in Liver Microsomes from Dogs, Rats and Humans

The *in vitro* phase I metabolism of enflicoxib was determined using [^{14}C]Enflicoxib as the substrate. The profile of enflicoxib phase I metabolism was characterized by the formation of three main metabolites that were named M7, M8 and E-6132. The analyses of liver microsomes incubated with radiolabeled [^{14}C]Enflicoxib showed no relevant amounts of other metabolites. In addition, no qualitative differences in the enflicoxib phase I metabolism profile were found among the three species tested. Fig. (**2**) shows the representative HPLC-rad profile of [^{14}C]Enflicoxib metabolism obtained for male Wistar rat liver microsomes at the incubation times of 0, 30, 60 and 90 min. Metabolite E-6132 showed very poor HPLC separation from unchanged enflicoxib under the conditions used for HPLC-rad profiling. In this case, the UV absorbance spectra helped to discriminate the two compounds, with maximum absorbance peaks at 313 nm for enflicoxib and 252 nm for E-6132, consistent with their respective pyrazoline and pyrazol core structures (Fig. (**2**), bottom). The analytical selectivity for enflicoxib and its phase I metabolites improved when using LC with detection by mass spectrometry (Fig. (**3**), upper panel). The elimination rate of enflicoxib and the formation rates of its three main metabolites, together with their relative percentage at 60 min of incubation, are shown in Table **1** and Fig. (**4**). The highest rate of enflicoxib elimination was found in human liver microsomes followed by rat and dog, which showed 2.2- and 8.6-fold lower values, respectively (Fig. **4A**). M8 was the most efficiently formed metabolite in the three species, with formation rates of 188.9, 87.7 and 23.7 pmol min^{-1} mg^{-1} in humans, rats, and dogs, respectively (representing 56.1%, 24.3% and 7.0% of total drug-related material expressed as a molar amount). The E-6132 metabolite ranked second with similar formation rates between humans and rats, and 14- to 19-fold lower rates in dog liver microsomes. Metabolite M7 showed similar formation rates in the rat and the dog and a 3-4-fold higher rate in humans. Its relative percentage at 60 min was well below 10% in all three species Table **1**.

Results are expressed as the mean of duplicate incubations of liver microsomes with 20 μM [^{14}C]-labeled enflicoxib and incubation times of 0, 30, 60 and 90 min. The enflicoxib transformation rates (substrate depletion) or metabolite formation rates were calculated after linear fitting of the concentration of each compound *vs*. the incubation time in the linear time range.

3.2. Assessment of Enflicoxib Metabolism in Rat and Dog Intestinal Microsomes

As in the case of liver, three metabolites were detected in intestinal microsomes matching the exact masses of M7, M8 and E-6132. The quantitative results are shown in Table **2** and Fig. (**4C**). The amount of unchanged enflicoxib was still close to 100% after 60 and 120 min of incubation. Therefore, the enflicoxib transformation rate was very low and could not be effectively calculated from substrate depletion data. The M8 and E-6132 formation rates were much lower than those found in the liver in both species. Contrary to the liver, higher metabolite formation rates were found in the dog than in the rat. Metabolite M7 was detected in the dog but not in rat intestinal microsomes.

Results are expressed as the mean of duplicate incubations of intestinal microsomes with 20 μM unlabeled enflicoxib at incubation times of 0, 60 and 120 min. The metabolite formation rate was calculated from the concentration of each compound after 120 min incubation. Metabolite M7 was only detected in dog intestinal microsomes but was not quantified because no standards were available.

3.3. Metabolism of Enflicoxib and E-6132 in Cryopreserved Hepatocytes from Rats and Dogs

To investigate the potential phase II biotransformation of enflicoxib, dog and rat cryopreserved hepatocytes in suspension were incubated separately with enflicoxib and the E-6132 metabolite.

As shown in Table **3**, eight metabolites were detected after incubation of enflicoxib with rat hepatocytes, matching the exact masses of M7, M8, E-6132, enflicoxib glucuronide, M8 glucuronide, E-6132 glucuronide, M7 glu-

curonide and M7 sulfate. Fig. (**3**) shows the representative LC-MS profile of enflicoxib phase I and II metabolites obtained in male rat hepatocytes at the incubation time of 180 min. No detectable amounts of M7 glucuronide or M7 sulfate were produced by dog hepatocytes.

Results in Table **3** are expressed mean LC-MS peak areas of duplicate incubations of cryopreserved hepatocytes with 20 μM unlabeled enflicoxib and 20 μM E-6132 at incubation times of 0, 120 and 180 min. Columns 7 and 8: mean metabolism rate of enflicoxib and E-6132 (substrate depletion).

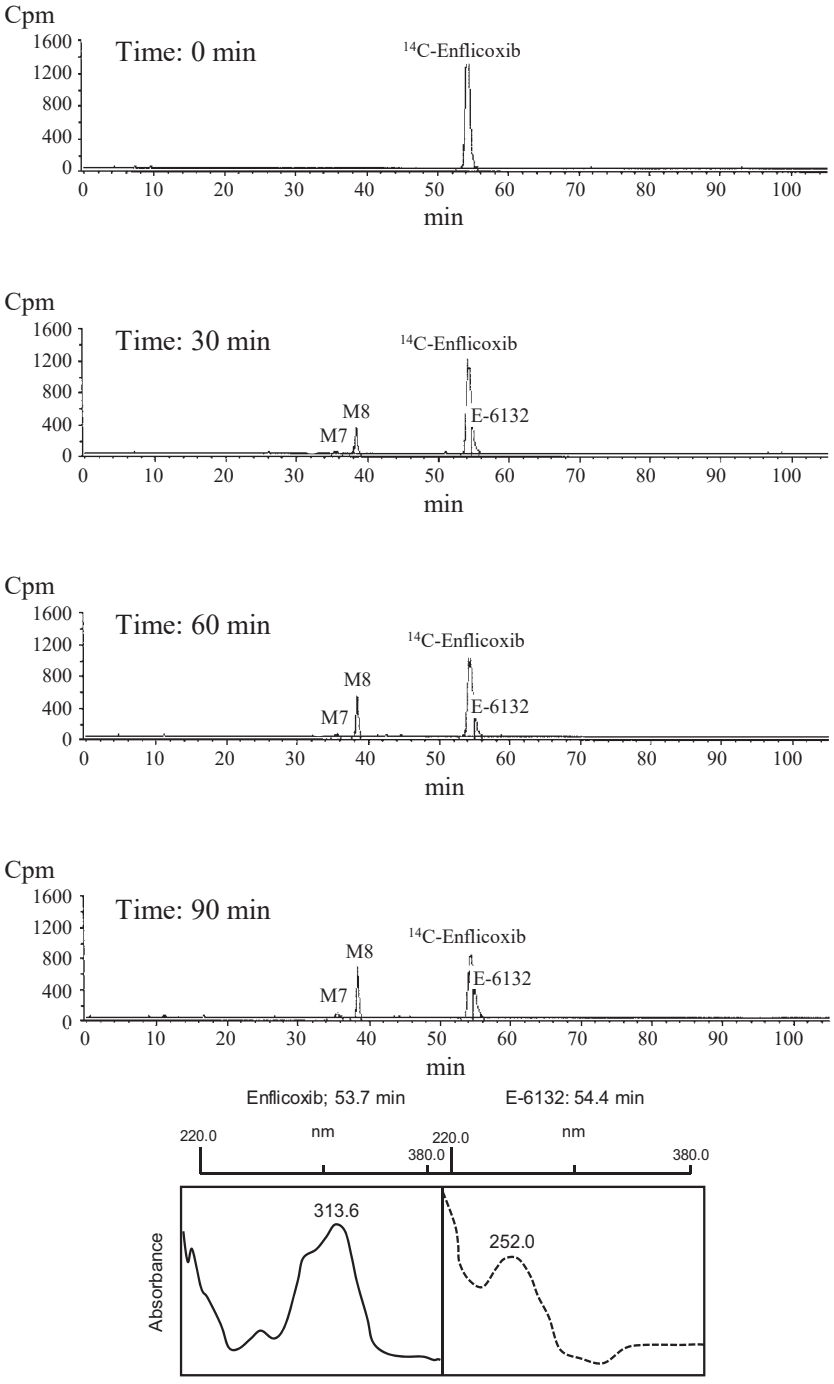

Fig. (2). Representative HPLC-rad profiles of *in vitro* metabolism of [^{14}C]Enflicoxib in pooled male rat liver microsomes after 0, 30, 60 and 90 min of incubation. cpm: on-line radioactivity detection units; Lower panel: UV absorbance spectra of enflicoxib and metabolite E-6132. (*A higher resolution version of this figure is available in the electronic copy of the article*).

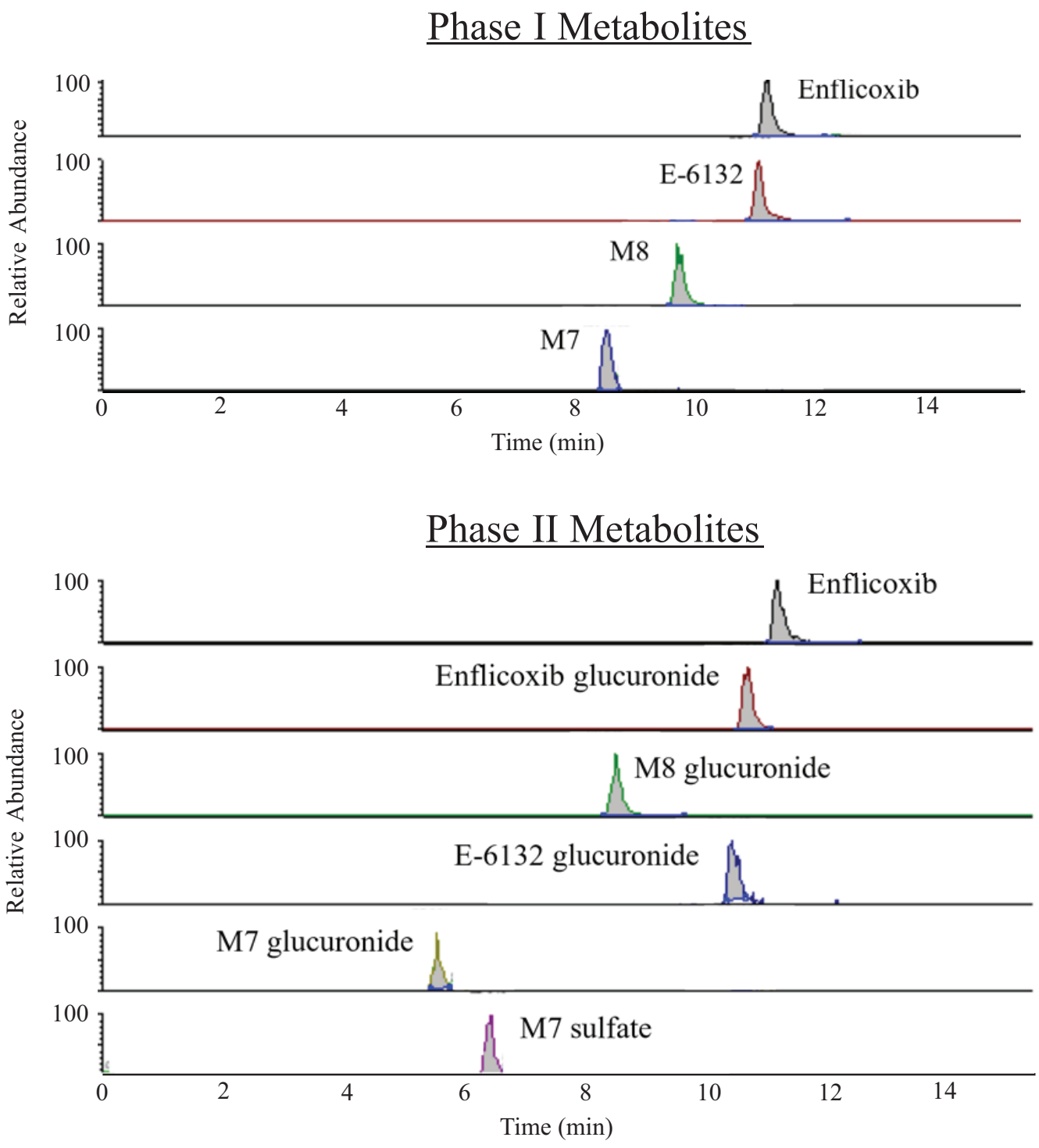

Fig. (3). Representative LC-MS profiles of *in vitro* metabolism of unlabeled enflicoxib. Upper panel: phase I metabolites formed by male Wistar rat liver microsomes after 90 min of incubation. Lower panel: phase II metabolites formed by male Wistar rat cryopreserved hepatocytes after 180 min of incubation. Relative abundance: on-line targeted MS normalized response. (*A higher resolution / colour version of this figure is available in the electronic copy of the article*).

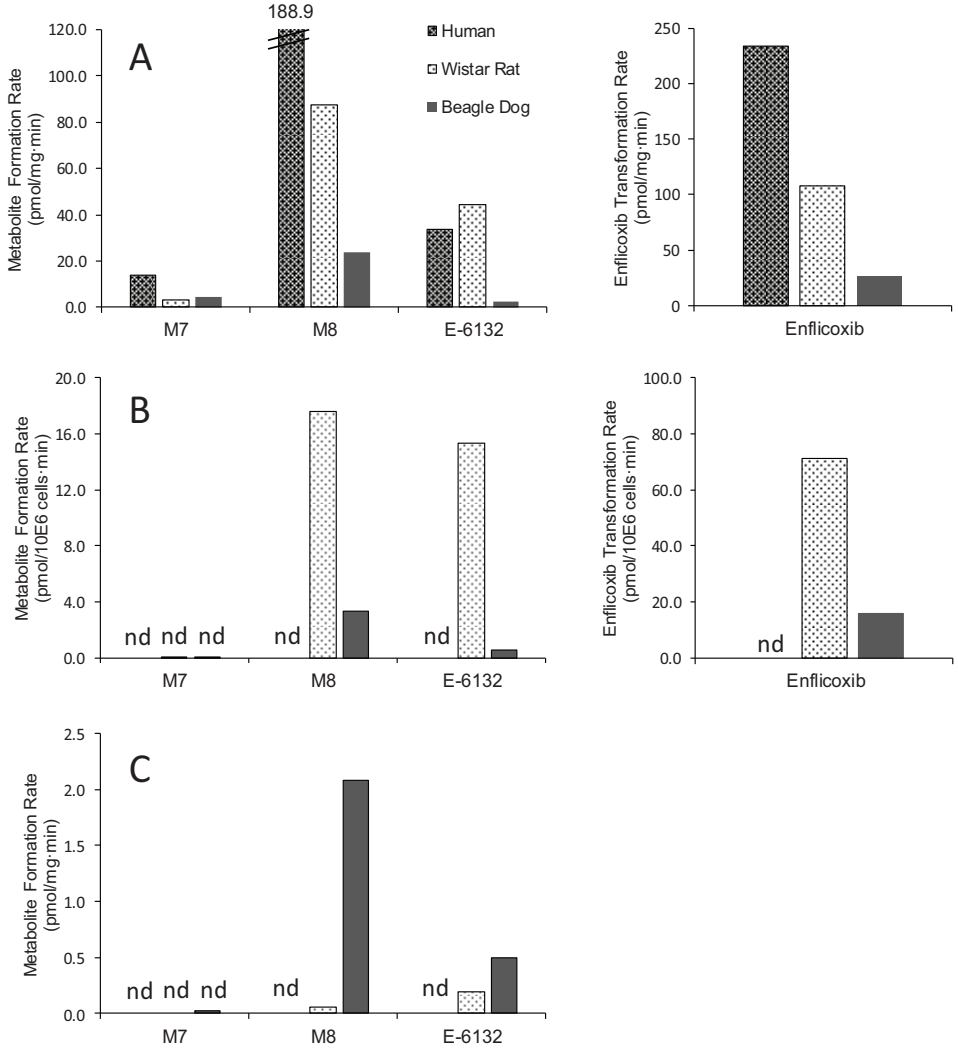

Fig. (4). Rate of enflicoxib metabolism (right panel) and formation of its two primary phase I metabolites M8 and E-6132 (left panel). Data correspond to liver microsomes (**A**), cryopreserved hepatocytes (**B**) and intestinal microsomes (**C**) from humans, rats and dogs. Results are the mean of duplicate experiments and are expressed as pmol min^{-1} mg^{-1} for liver and intestine microsomes or pmol $(min \cdot 10^6 \text{ cells})^{-1}$ for cryopreserved hepatocytes. nd: not determined. (*A higher resolution / colour version of this figure is available in the electronic copy of the article*).

Table 1. Metabolism of enflicoxib in liver microsomes from rats, dogs and humans.

Metabolite	Parameter	Species			Ratio Dog/Rat
		Wistar Rat	Beagle Dog	Human	
Enflicoxib	*Relative %*	62.4	91.0	29.7	-
	Rate	108.2†	26.9†	233.4*	0.25
M7	*Relative %*	0.89	1.3	4.2	-
	Rate	3.2†	4.3†	14.0*	1.34
M8	*Relative %*	24.3	7.0	56.1	-
	Rate	87.7†	23.7†	188.9*	0.27
E-6132	*Relative %*	12.3	0.7	10.0	-
	Rate	44.5†	2.4†	33.7*	0.05

Metabolism rate is expressed as pmol min^{-1} mg^{-1}

*† Rate calculated for the time range 0-30 min.

† Average of rates calculated for the time ranges 0-90 and 0-60 min.

Relative %: molar amount expressed as a percentage of parent enflicoxib after 60 min incubation.

Table 2. Metabolism of enflicoxib in intestinal microsomes from rats and dogs.

Metabolite	Parameter	Species		Ratio Dog/Rat
		Wistar Rat	Beagle Dog	
Enflicoxib	Relative %	99.86	98.27	-
	Rate	*nd*	*nd*	*nd*
M8	Relative %	0.03	1.38	-
	Rate	0.06	2.08	37.0
E-6132	Relative %	0.11	0.33	-
	Rate	0.19	0.50	2.6

nd not determined
Rate calculated for the time range 0-120 min (pmol min^{-1} mg^{-1})
Relative % (120 min): molar amount expressed as percentage of parent enflicoxib after 120 mi. incubation

Table 3. Profile of enflicoxib metabolites in cryopreserved hepatocytes from rats and dogs.

Metabolite	Time (min)	LC-MS Peak Area				Metabolism Rate pmol $(min \cdot 10^6 cells)^{-1}$	
		Substrate: Enflicoxib		*Substrate*: E-6132			
		Wistar Rat	Beagle Dog	Wistar Rat	Beagle Dog	Rat	Dog
Unchanged enflicoxib	0	1368 *(20)*	1377 *(20)*	0	0	88.5*	-
	120	642 *(9.4)*	1415 *(20.5)*	0	0		15.7*
	180	492 *(7.2)*	1182 *(17.2)*	0	0		
M7	0	0	0	0	0	-	-
	120	2	0	0	0	-	-
	180	1	1	0	0	-	-
M8	0	0	0	0	0	-	-
	120	1445	196	0	0	-	-
	180	1411	266	0	0	-	-
E-6132	0	0	0	16180 *(20)*	18247 *(20)*	-	-
	120	2030	58	16575 *(20.5)*	17449 *(19.1)*	23.4†	*nd*
	180	2171	77	12771 *(15.8)*	18883 *(20.7)*	-	-
M7 Sulfate	0	0	0	0	0	-	-
	120	9	0	0	0	-	-
	180	11	0	0	0	-	-
M7 Glucuronide	0	0	0	0	0	-	-
	120	9	0	0	0	-	-
	180	11	0	0	0	-	-
M8 Glucuronide	0	0	0	0	0	-	-
	120	109	< 1	0	0	-	-
	180	154	< 1	0	0	-	-
E-6132 Glucuronide	0	0	0	0	0	-	-
	120	7	0	141	1	-	-
	180	13	0	170	1	-	-
Enflicoxib Glucuronide	0	0	0	0	0	-	-
	120	119	1	0	0	-	-
	180	131	1	0	0	-	-

nd not determined
* transformation rate calculated for the time range 0-120 minutes
† transformation rate calculated for the time range 0-180 minutes
In parentheses concentration of substrate remaining (μM)

Table 4. Secondary metabolism of M8 and E-6132 metabolites in liver microsomes from rats and dogs.

Metabolite	Time (min)	LC-MS Peak Area			
		Substrate: M8		*Substrate*: E-6132	
		Wistar Rat	Beagle Dog	Wistar Rat	Beagle Dog
Unchanged enflicoxib	0	0	0	0	0
	60	0	0	0	0
	120	0	0	0	0
M7	0	0	0	0	0
	120	3.04	1.31	0	0
	180	2.93	1.68	0	0
M8	0	81.35	87.95	0	0
	120	81.51	90.49	0	0
	180	89.97	97.61	0	0
E-6132	0	0	0	148.23	122.31
	120	0	0	128.54	128.65
	180	0	0	152.20	149.00

E-6132 glucuronide was the sole metabolite formed in both species when E-6132 was used as substrate instead of enflicoxib. The total transformation rates for enflicoxib or E-6132 (when used as substrate) were calculated from substrate depletion. As shown in Table **3**, enflicoxib was transformed in rat hepatocytes at a faster rate than in dog hepatocytes. The E-6132 transformation rate was 23.4 pmol $(min \cdot 10^6 \text{ cells})^{-1}$ in rats. However, in dog hepatocytes, it could not be efficiently calculated because the amount of unchanged substrate after incubation was nearly the same as in T=0 samples. The formation rates of M8 and E-6132 from enflicoxib were also determined and are depicted graphically in Fig. (**4B**). As for liver microsomes, M8 and E-6132 formation was higher in rats than in dogs.

3.4. Assessment of the Secondary Phase I Metabolism of Enflicoxib in Liver Microsomes - Characterization of the Metabolic Pathway of M7 Formation

The potential secondary phase I transformation of metabolites M8 and E-6132, and the possible formation pathways of metabolite M7 were assessed in incubations of dog and rat liver microsomes with M8 or E-6132. As shown in Table **4**, metabolite M7 was formed after incubation of metabolite M8 with liver microsomes from both species. The peak area of M8 substrate did not show any evident decrease after the incubation period, meaning that the rate of M7 formation was very low in both species. No other known metabolites were formed in the microsomal incubations with M8. The M7 structure was tentatively identified by LC-MS (supplementary material). The results of these analyses indicate a molecular structure for metabolite M7 consistent with the presence of a hydroxylated pyrazol moiety Fig. (**5**). Finally, metabolite E-6132 was not secondarily metabolized by phase I enzymes in liver microsomes (Table **4**).

Results are expressed as mean LC-MS peak area of duplicate incubations of liver microsomes with 20 μM unlabeled substrate at incubation times of 0, 60 and 120 min.

3.5. Metabolism Positive Controls

The positive metabolism control results Table **5** correlated with the capacity of rats and dogs to metabolize enflicoxib in the different experimental systems and confirmed their metabolic competence. Testosterone elimination showed half-lives of 2.4, 133.3 or <10 min in rat liver and intestinal microsomes or hepatocytes, respectively. In the dog, the respective testosterone half-lives were 25.5, 35.5 and <10 min. The phase II competence of hepatocytes was also evaluated (7-hydroxy-4-methylcoumarin elimination). The results are also shown in Table **5**.

4. DISCUSSION

Enflicoxib was efficiently metabolized *in vitro* in dogs, rats, and humans. Three main phase I metabolites were detected, accounting for most of the fraction metabolized in liver microsomes as demonstrated in incubations with the ^{14}C-labeled analogue of enflicoxib. These metabolites were named M7, M8 and E-6132. Metabolites M8 and E-6132 were previously identified as hydroxy-pyrazoline and pyrazol derivatives of the parent compound, respectively [9]. Moreover, the results shown as supplementary material in the present work indicate that the chemical modifications involved in the formation of M7 are oxidation of enflicoxib's pyrazoline ring leading to the hydroxylated pyrazol structure shown in Fig. (**5**). Since the same qualitative profile of enflicoxib phase I metabolism was essentially produced in dogs, rats and humans, no concerns are expected regarding the selection of the rat as the toxicological species. In addition, exposure to different / unique phase I metabolites is not anticipated in humans in case of accidental ingestion [11].

Based on the enflicoxib metabolic elimination rate in liver microsomes, the species could be ranked as follows: human > rat > dog. The metabolite M8 accounted for most of the metabolized fraction of enflicoxib in the three species. The ratio of metabolite M8 formation rate in dogs *vs*. rats was 0.27, which is very close to the ratio of the total enfli-

Table 5. Half-life of testosterone (phase I metabolism control) and 7-hydroxy-4-methylcoumarin (phase II metabolism control) elimination in the different experimental systems used in the study.

Species	Substrate	Test System	*K*	$t_{1/2}$ *(min)*
Rat	Testosterone	Liver microsomes*	-0.2830	2.4
		Liver microsomes†	-0.3314	2.1
		Intestinal microsomes	-0.0052	133.3
		Hepatocytes	nd	< 4.7
Dog	Testosterone	Liver microsomes*	-0.0271	25.5
		Liver microsomes†	-0.0231	30.0
		Intestinal microsomes	-0.0195	35.5
		Hepatocytes	-0.0914	7.6
Rat	7-hydroxy-4-methylcoumarin	Hepatocytes	nd	< 5.9
Dog	7-hydroxy-4-methylcoumarin	Hepatocytes	-0.0658	10.5

$t_{1/2} = 0.693/K$
nd not determined (below the lower limit of quantitation)
* experiments corresponding to incubations with enflicoxib as substrate
† *experiments corresponding to incubations with M8 as substrate*

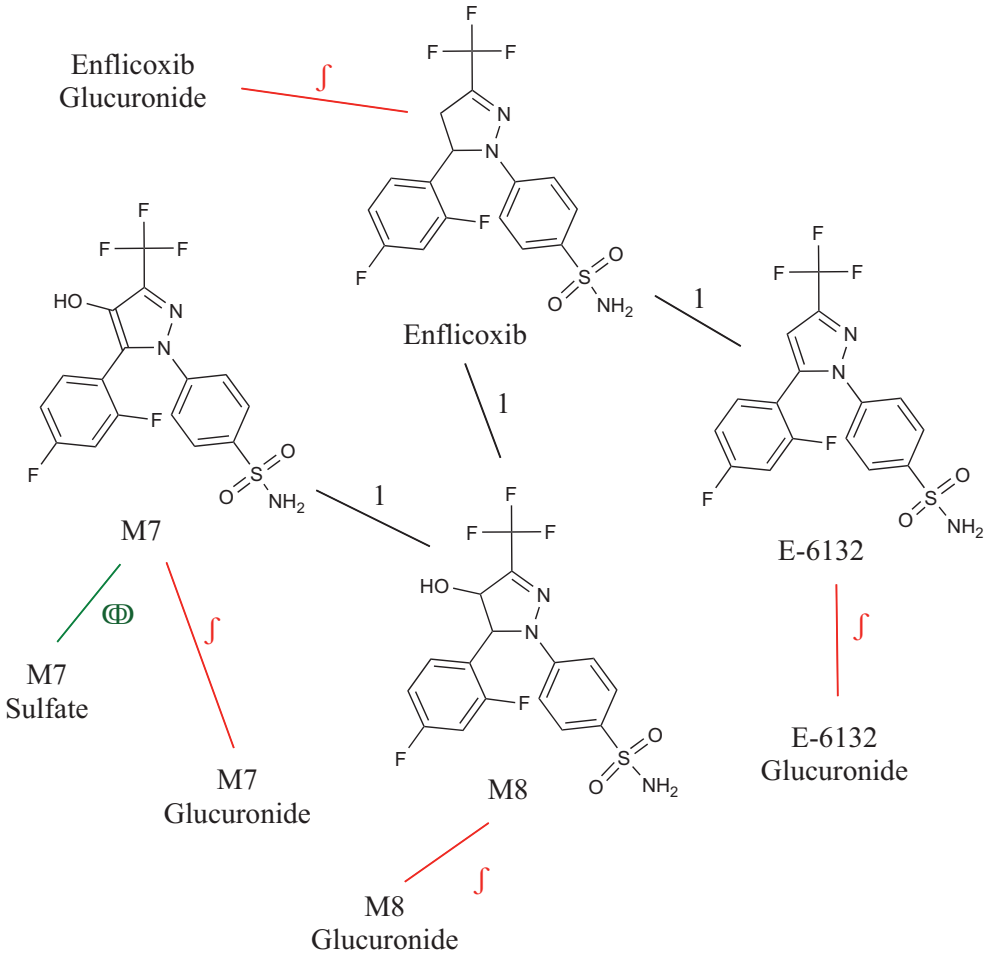

Fig. (5). Enflicoxib metabolites formed *in vitro* and proposed enzymatic pathways in dogs and rats. 1: cytochrome P-450 enzymes, 2: UDP-glucuronosyl transferases, 3: sulfotransferases. Red: reactions present in rats and dogs; Green: reaction found only in rats. (*A higher resolution / colour version of this figure is available in the electronic copy of the article*).

coxib transformation rate (0.25) for both species, meaning that M8 formation is actually driving most of the phase I enflicoxib metabolism. The active enflicoxib metabolite E-6132 showed comparatively slow formation rates, especially in dogs, thus potentially being predictive of the actual situation *in vivo* and suggesting the slow transformation of the parent compound through this pathway in the target species. The formation rates of M7 in liver microsomes usually paralleled those of M8, suggesting that M7 might actually be an M8 metabolite. This was further corroborated in incubations of M8 with liver microsomes from dogs and rats, where M7 was effectively formed Table **4**. On the contrary, when the pyrazol metabolite E-6132 was incubated with liver microsomes, no known enflicoxib metabolites were formed. Altogether, these results indicate that M7 is a secondary enflicoxib metabolite formed by oxidation of M8 but not by hydroxylation of E-6132. The results from incubations in the absence of NADPH cofactor showed no transformations (data not shown), indicating the likely involvement of cytochrome P-450 enzymes in the formation of M8, E-6132 and M7.

Because enflicoxib is intended for oral administration, the potential extra-hepatic metabolism of enflicoxib in the gut was assessed in incubations with intestinal microsomes. While the metabolite profile was qualitatively similar to liver microsomes, the intestinal microsomes showed a very low capacity to metabolize enflicoxib. This was particularly evident when calculating M8 and E-6132 formation rates (Table **2**), which were several times lower than those in liver. Altogether, these results indicate that an intestinal first pass of enflicoxib in the dog is unlikely *in vivo*.

The main enflicoxib metabolite M8 contains two chiral centers and, therefore, two racemic stereoisomers are chemically possible. In the different experiments in the present work, metabolite M8 co-eluted in the HPLC analyses with the M8-anti diastereoisomer authentic standard (mixture of 4R-difluorophenyl/5R-dihydro-pyrazol and 4S-difluorophenyl/5S-dihydro-pyrazol). Given M8's lack of pharmacologic activity, the characterization of the enantiomeric composition of metabolite M8 was not considered relevant.

To complete the assessment of enflicoxib metabolism, enflicoxib and its pyrazol metabolite E-6132 were incubated with rat and dog hepatocytes. The results of these experiments revealed the formation of five phase II metabolites: enflicoxib glucuronide, M8 glucuronide, E-6132 glucuronide, M7 glucuronide, and M7 sulfate. The latter two were not detected in the dog incubates. These results demonstrate that unchanged enflicoxib can be primarily eliminated by conjugation with glucuronic acid, and the remaining phase I metabolites also undergo secondary glucurono-conjugation. The conjugation sites were not assessed experimentally; however, two nucleophilic groups are susceptible to this reaction, namely, the amine of the sulphonamide moiety of enflicoxib and its metabolites, and the hydroxyl group at the pyrazoline ring of metabolite M8 and at the pyrazol ring of metabolite M7.

Of special interest was the assessment of the potential metabolic elimination of metabolite E-6132, not only because of its observed long-lasting pharmacokinetics but also because the *in vivo* pharmacological activity of enflicoxib has been attributed to this metabolite [7]. The results of the present work strongly suggest that E-6132 is eliminated by a single pathway comprising conjugation with glucuronic acid. The rate of E-6132 glucuronidation in dog hepatocytes was considerably low (Table **3**). Therefore, E-6132 showed low rates of formation and also of elimination in dogs. The balance between these rates underlies the mechanism explaining the long half-life of E-6132 *in vivo*. Since the major route of excretion of enflicoxib and its metabolites is in bile [12], a putative entero-hepatic recirculation effect could also contribute to the long-lasting pharmacokinetics of E-6132.

The biotransformation of enflicoxib showed specific features when compared to other coxibs, being their metabolic pathways clearly dependent on the chemical structures of the different drugs. The sulphamoil substituted coxibs, such as celecoxib (pyrazol), cimicoxib (imidazol) and valdecoxib (isoxazol), undergo phase I dealkylation or oxidation followed by phase II glucuronidation [13-15]. Meanwhile, the furanone-based sulfonylphenyl coxib, such as rofecoxib, seems more prone to reduction-based reactions [16], although dealkylation and glucuronidation are also described for firocoxib, a drug of the same chemical family [17]. Indeed, the most remarkable difference between enflicoxib and the other mentioned coxibs still relies on the fact that, for enflicoxib, one of its main metabolites is actually responsible for most of the pharmacological activity.

CONCLUSION

In conclusion, phase I metabolism of enflicoxib was qualitatively very similar among rats, humans, and the target species, dogs. Three main metabolites (M7, M8, and E-6132) account for almost all the fractions metabolized in liver microsomes, and their chemical structures are already identified. These findings support the selection of rats as the species for toxicological evaluation. In addition, no unique or disproportionate phase I metabolites were formed in humans. For this reason, no differential metabolism is expected in humans in case of accidental ingestion. Metabolite M8 can be considered the major metabolite, but there is experimental evidence indicating that M8 is not an active metabolite. Metabolite M7 is derived from the oxidation of M8. On the other hand, the active metabolite E-6132 is formed at a very low rate and is eliminated most probably by a single mechanism consisting of conjugation with glucuronic acid, a reaction that also shows a very low rate. The slow formation and elimination rates of E-6132 underlie the metabolic mechanism for its long-lasting pharmacokinetics and enflicoxib's overall sustained efficacy.

LIST OF ABBREVIATIONS

CID	= Collision-induced Dissociation
COX	= Cyclooxygenase
COX-1	= Cyclooxygenase Isozyme-1

COX-2	=	Cyclooxygenase Isozyme-2
CID	=	Collision-induced Dissociation
CYP	=	Cytochrome P450
DMSO	=	Dimethylsulfoxide
ESI	=	Electrospray Ionization
FA	=	Formic Acid
HPLC	=	High Performance Liquid Chromatography
HPLC-rad	=	high Performance Liquid Chromatography Coupled with Radioactivity Detection
LC-MS	=	liquid Chromatography Coupled with Mass Spectrometry Detection
LTQ	=	Linear ion Trap
MW	=	Molecular Weight
NADP/NADPH	=	Nicotinamide Adenine Dinucleotide Phosphate Oxidized/reduced Forms
UV	=	Ultra-violet

ETHICS APPROVAL AND CONSENT TO PARTICIPATE

Not applicable.

HUMAN AND ANIMAL RIGHTS

Not applicable.

CONSENT FOR PUBLICATION

Not applicable.

AVAILABILITY OF DATA AND MATERIALS

The data that support the findings of this study are available from the corresponding author, [JH], upon reasonable request.

FUNDING

This work was financially supported by Ecuphar/Animalcare Group *via* contracted research studies.

CONFLICT OF INTEREST

J. Homedes and M. Salichs are employees of Ecuphar Veterinaria S.L.U. (Animalcare Group plc), who funded this project. J. Solà and À. Menargues conducted the research funded by Ecuphar Veterinaria S.L.U. (Animalcare Group plc). M.T. Serafini and G. Encina declare no conflict of interest.

ACKNOWLEDGEMENTS

The authors thank Eliandre De Oliveira, M. Antònia Odenas and Santiago Puig, for their technical assistance.

SUPPLEMENTARY MATERIAL

In vitro metabolite M7 generation and LC-MS analysis for tentative chemical identification

REFERENCES

[1] European Commission Union Register of veterinary medicinal products. Daxocox. 2021. Available from: https://ec.europa.eu/health/documents/community-register/html/v270.htm [Accessed on: Jun 15, 2021].

[2] Wagemakers, M.; van der Wal, G.E.; Cuberes, R.; Alvarez, I.; Andrés, E.M.; Buxens, J.; Vela, J.M.; Moorlag, H.; Mooij, J.J.; Molema, G. COX-2 inhibition combined with radiation reduces orthotopic glioma outgrowth by targeting the tumor vasculature. *Transl. Oncol.,* **2009**, *2*(1), 1-7. http://dx.doi.org/10.1593/tlo.08160 PMID: 19252746

[3] Iñiguez, M.A.; Punzón, C.; Cacheiro-Llaguno, C.; Díaz-Muñoz, M.D.; Duque, J.; Cuberes, R.; Alvarez, I.; Andrés, E.M.; Buxens, J.; Buschmann, H.; Vela, J.M.; Fresno, M. Cyclooxygenase-independent inhibitory effects on T cell activation of novel 4,5-dihydro-3 trifluoromethyl pyrazole cyclooxygenase-2 inhibitors. *Int. Immunopharmacol.,* **2010**, *10*(10), 1295-1304. http://dx.doi.org/10.1016/j.intimp.2010.07.013 PMID: 20709632

[4] Orjales, A.; Mosquera, R.; López, B.; Olivera, R.; Labeaga, L.; Núñez, M.T. Novel 2-(4-methylsulfonylphenyl)pyrimidine derivatives as highly potent and specific COX-2 inhibitors. *Bioorg. Med. Chem.,* **2008**, *16*(5), 2183-2199. http://dx.doi.org/10.1016/j.bmc.2007.11.079 PMID: 18158247

[5] Pavase, L.S.; Mane, D.V.; Bahetib, K.G. Anti-inflammatory exploration of Sulfonamide containing Diaryl Pyrazoles with promising COX-2 selectivity and enhanced gastric safety profile. *J. Heterocycl. Chem.,* **2018**, *55*, 913-922. http://dx.doi.org/10.1002/jhet.3118

[6] Calvet, C.; Cuberes, R.; Pérez-Maseda, C.; Frigola, J. Enantioseparation of novel COX-2 anti-inflammatory drugs by capillary electrophoresis using single and dual cyclodextrin systems. *Electrophoresis,* **2002**, *23*(11), 1702-1708. http://dx.doi.org/10.1002/1522-2683(200206)23:11<1702::AID-ELPS1702>3.0.CO;2-# PMID: 12179991

[7] Reinoso, R.F.; Farrán, R.; Moragón, T.; García-Soret, A.; Martínez, L. Pharmacokinetics of E-6087, a new anti-inflammatory agent, in rats and dogs. *Biopharm. Drug Dispos.,* **2001**, *22*(6), 231-242. http://dx.doi.org/10.1002/bdd.258 PMID: 11754039

[8] Homedes, J.; Salichs, M.; Solà, J.; Menargues, A.; Cendrós, J-M.; Encina, G. Pharmacokinetics of enflicoxib in dogs: Effects of prandial state and repeated administration. *J. Vet. Pharmacol. Therap.,* **2021**, 1-14. http://dx.doi.org/10.1111/jvp.12995

[9] Pretel, M.J.; Serafini, M.T.; Port, A.; Cuberes, R.; Frigola, J.; Martinez, L. E-6232 Metabolism. *Drug Metab. Rev.,* **2001**, *33*(Suppl. 1), 116.

[10] Woodward, K.N. Assessment of user safety, exposure and risk to veterinary medicinal products in the European Union. *Regul. Toxicol. Pharmacol.,* **2008**, *50*(1), 114-128. http://dx.doi.org/10.1016/j.yrtph.2007.10.007 PMID: 18060673

[11] European Agency for the Evaluation of Medicinal Products. Guideline on user safety for pharmaceutical veterinary medicinal products. 2010. Available from: https://www.ema.europa.eu/en/documents/scientific-guideline/guideline-user-safety-pharmaceutical-veterinary-medicinal-products_en.pdf [Accessed on: Jun 07, 2021].

[12] Serafini, M.T.; Reinoso, R.F.; Moragón, T.; García-Soret, A.; Carreras, J.; Puig, S. Disposition of [^{14}C]E-6232 in rat. *Drug Metab. Rev.,* **2001**, *33*(Suppl. 1), 119.

[13] Subhahar, M.B.; Singh, J.; Albert, P.H.; Kadry, A.M. Pharmacokinetics, metabolism and excretion of celecoxib, a selective cyclooxygenase-2 inhibitor, in horses. *J. Vet. Pharmacol. Ther.,* **2019**, *42*(5), 518-524. http://dx.doi.org/10.1111/jvp.12757 PMID: 30888074

[14] Schneider, M.; Dron, F.; Cuinet, E.; Woehrlé, F. Comparative

pharmacokinetic profile of cimicoxib in dogs and cats after IV administration. *Vet. J.,* **2021**, *270 120625*, 1-5. http://dx.doi.org/10.1016/j.tvjl.2021.105625

[15] Zhang, J.Y.; Yuan, J.J.; Wang, Y-F.; Bible, R.H., Jr; Breau, A.P.; Breau, A. Pharmacokinetics and metabolism of a COX-2 inhibitor, valdecoxib, in mice. *Drug Metab. Dispos.,* **2003**, *31*(4), 491-501. http://dx.doi.org/10.1124/dmd.31.4.491 PMID: 12642477

[16] Slaughter, D.; Takenaga, N.; Lu, P.; Assang, C.; Walsh, D.J.; Arison, B.H.; Cui, D.; Halpin, R.A.; Geer, L.A.; Vyas, K.P.; Baillie, T.A. Metabolism of rofecoxib *in vitro* using human liver subcellular fractions. *Drug Metab. Dispos.,* **2003**, *31*(11), 1398-1408. http://dx.doi.org/10.1124/dmd.31.11.1398 PMID: 14570773

[17] Kvaternick, V.; Pollmeier, M.; Fischer, J.; Hanson, P.D. Pharmacokinetics and metabolism of orally administered firocoxib, a novel second generation coxib, in horses. *J. Vet. Pharmacol. Ther.,* **2007**, *30*(3), 208-217. http://dx.doi.org/10.1111/j.1365-2885.2007.00840.x PMID: 17472652